Out-of-plane conductivity for quantum wells in a parallel magnetic field

2000 J. Phys.: Condens. Matter 12 1789

(http://iopscience.iop.org/0953-8984/12/8/320)

J. Phys.: Condens. Matter **12** (2000) 1789–1796. Printed in the UK PII: S0953-8984(00)05674-5

Out-of-plane conductivity for quantum wells in a parallel magnetic field

Godfrey Gumbs†

Department of Physics and Astronomy, Hunter College of the City University of New York, 695 Park Avenue, New York, NY 10021, USA

Received 5 June 1999, in final form 7 January 2000

Abstract. The out-of-plane static magnetoconductivity $\sigma_\perp$ is calculated as a function of temperature for a single quantum well and a double quantum well in the presence of a parallel magnetic field. The effects of the extended states above the top of the potential barrier are included in the calculations of the temperature dependence. The electron tunnelling between wells is shown to enhance $\sigma_\perp$ as the temperature is increased. At low temperatures ($T \ll T_F$), the variation of $\sigma_\perp$ with temperature is determined by the electron density.

1. Introduction

In a double-quantum-well (DQW) structure, the tunnelling between the two parallel two-dimensional electron gas (2DEG) layers introduces several interesting features in the cyclotron resonance [1] and magnetoplasmon excitation spectrum [2, 3] as well as the electrical transport [4], all of which have no counterpart in a single 2DEG. For example, in the far-infrared experiments of Arnone *et al* [1], it was shown that the cyclotron resonance transitions in the presence of a parallel magnetic field reveal anticrossing between the Landau levels associated with different subbands of strongly coupled 2DEGs. The dispersion relations for strongly coupled quantum wells with tunnelling have an in-phase (symmetric) and an out-of-phase (antisymmetric) plasmon mode. The effect due to tunnelling could of course be adjusted by varying the thickness of the barrier layer separating the two quantum wells. As reported recently, the role of tunnelling has also been demonstrated in theoretical calculations of the magnetoplasmon excitation for a magnetic field perpendicular to the 2DEG layers (see reference [3] and references cited therein). In a series of papers, Simmons *et al* [5–7] and Lyo [8] have reported on experiments on the conductivity and cyclotron resonance for DQW structures when a magnetic field is applied parallel to the 2D planes. In reference [6], the magnetic field $\boldsymbol{B}_\parallel$ is in the z-direction, the electron gases are in the y–z plane, and the electric field $\boldsymbol{E}$ makes an angle θ with $\boldsymbol{B}_\parallel$. The component of the current $\boldsymbol{j}$ in the direction of $\boldsymbol{E}$ yields the in-plane magnetoconductivity $\boldsymbol{j}\cdot\boldsymbol{E}/E^2$ which exhibits several novel phenomena due to anticrossing of the electron energy dispersion bands of the two QWs in the presence of an in-plane magnetic field [8]. Resonant tunnelling experiments have also been reported for DQWs in a parallel magnetic field [9]. These experiments show the effect due to tunnelling on the current–voltage characteristics. Zheng and MacDonald [10] have calculated the magnetic

† Also at: The Graduate School and University Center of the City University of New York, 365 Fifth Avenue, New York, NY 10036, USA.

0953-8984/00/081789+08$30.00

field dependence of the low-temperature tunnelling conductance for a DQW structure in a parallel magnetic field.

In this paper, we are interested in calculating the static conductivity $\sigma_\perp$ for a single quantum well (SQW) and a DQW with the magnetic field in the plane of the 2DEG. In our calculations, we determine the tunnelling conductance over a wide range of temperature and include the extended states above the top of the well in addition to the confined states within the well since the contribution to the conductivity from the higher-lying states cannot be neglected at finite temperature.

2. Energy eigenstates

Let us first consider electrons moving in the y–z plane in a magnetic field $\boldsymbol{B}_\parallel$ parallel to the z-axis and a one-dimensional potential $U_{ext}(x)$. In the Landau gauge with vector potential $\boldsymbol{A} = (0, B_\parallel x, 0)$, the Schrödinger equation for an electron with effective mass m^* has the form

$$\left[-\frac{\hbar^2}{2m^*}\frac{\partial^2}{\partial x^2} - \frac{\hbar^2}{2m^*}\frac{\partial^2}{\partial z^2} + \frac{1}{2m^*}\left(-\mathrm{i}\hbar\frac{\partial}{\partial y} + eB_\parallel x\right)^2 + U_{ext}(x)\right]\psi_{j\boldsymbol{k}_\parallel}(\boldsymbol{r}) = E_j(\boldsymbol{k}_\parallel)\psi_{j\boldsymbol{k}_\parallel}(\boldsymbol{r}) \tag{1}$$

where j is a quantum number labelling the subbands and $\boldsymbol{k}_\parallel = (k_y, k_z)$. We note that for a symmetric potential with $U_{ext}(-x) = U_{ext}(x)$, for $x \to -x$ the Hamiltonian in this gauge is invariant under $B_\parallel \to -B_\parallel$. For equation (1), we write the wave function in the form of $\psi_{j\boldsymbol{k}_\parallel}(\boldsymbol{r}) = \phi_{jk_y}(x)\exp(\mathrm{i}k_y y + \mathrm{i}k_z z)/\sqrt{A}$, where A is the cross-sectional area of the 2DEG, and we introduce a new variable $\xi_{k_y} = \sqrt{2}(x/\ell_\mathrm{H} + \ell_\mathrm{H}k_y)$. Then, equation (1) yields

$$\frac{\partial^2\phi_{jk_y}(\xi_{k_y})}{\partial\xi_{k_y}^2} + \left[\frac{E_j(k_y) - U_\mathrm{ext}(\xi_{k_y})}{\hbar\omega_c} - \frac{\xi_{k_y}^2}{4}\right]\phi_{jk_y}(\xi_{k_y}) = 0 \tag{2}$$

where $E_j(k_y) = E_j(\boldsymbol{k}_\parallel) - \hbar^2k_z^2/2m^*$, $\omega_c = eB_\parallel/m^*$, and $\ell_\mathrm{H} = \sqrt{\hbar/eB_\parallel}$ is the magnetic length. When U_ext in equation (2) is a constant, we have the standard equation for parabolic cylinder functions [11, 12]. Subsequently, for the DQW, the general solution of equation (2) can be expressed in terms of two linearly independent parabolic cylinder functions $D_\nu(\xi_{k_y})$ and $V_\nu(\xi_{k_y})$ [13], where $\nu = [E_j(k_y) - E_0]/\hbar\omega_c - 1/2$, with $E_0 = 0$ or V_0 in the well or barrier region, respectively, of the QW.

In figure 1(a), we present results for the scaled energy eigenvalues $\nu_0 = E_j(k_y)/\hbar\omega_c - 1/2$ in a SQW, obtained by solving equation (2), as a function of the parallel magnetic field $B_\parallel$. Here, we take $\boldsymbol{k}_\parallel = 0$, and use the parameters appropriate to GaAs/AlGaAs, i.e., $m^* = 0.067\ m_e$ where m_e is the free-electron mass. The well has zero potential for $-a < x < a$ and we take the well width $2a = 200$ Å, and the height of the barrier outside the well is $V_0 = 213$ meV. In figure 1(b), we display the energy eigenvalues in the SQW as a function of k_y for a parallel magnetic field $B_\parallel = 4$ T and $k_z = 0$. All the other parameters for the quantum well are the same as for figure 1(a).

In figures 2(a) and 2(b), we plot the scaled energy eigenvalues $\nu_0 = E_j(k_y)/\hbar\omega_c - 1/2$ in a DQW by solving equation (2) as a function of the parallel magnetic field $B_\parallel$ and the wave vector $\boldsymbol{k}_\parallel$, respectively. Each well has width $2a$ and the barrier between them is defined by $-b/2 < x < b/2$. In the region $x_1 < -(2a + b/2)$, the barrier has height V_0. In the second region $-(2a + b/2) < x < -b/2$, there is a quantum well with $E_0 = 0$. In the region $-b/2 < x < b/2$, there is a potential barrier with $E_0 = V_0$. For $b/2 < x < (2a + b/2)$, there is a quantum well with $E_0 = 0$, and for $x > (2a + b/2)$, there is a barrier with $E_0 = V_0$. Here, we consider GaAs/AlGaAs and choose m^* and $2a$ to be the same as for figure 1; the

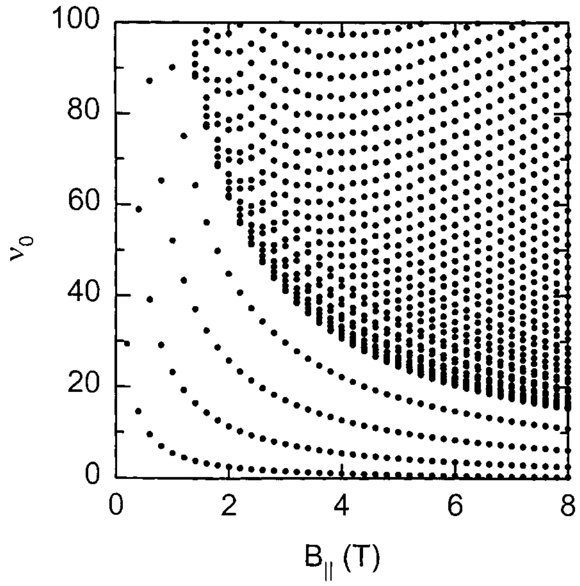

(a)

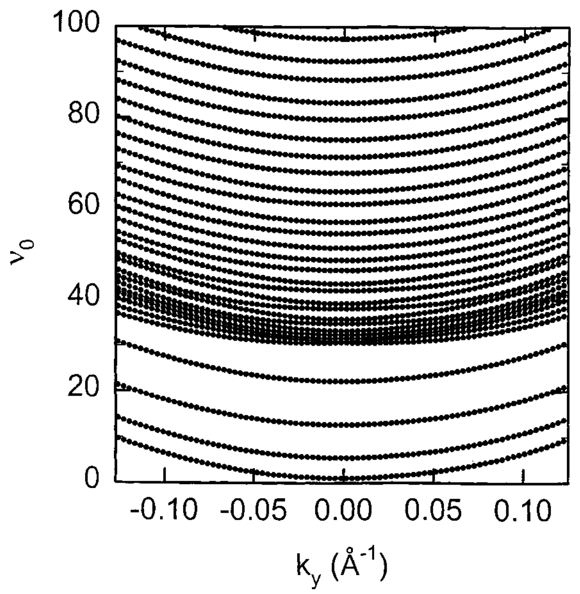

(b)

Figure 1. (a) A plot of the lowest, scaled energy eigenvalues $\nu_0 = E_j(k_y)/\hbar\omega_c - 1/2$ as a function of $B_\parallel$ for a single quantum well. We chose $k_y = 0$, $m^* = 0.0667\ m_e$, where m_e is the free-electron mass, the barrier height $V_0 = 213$ meV, and the well width $2a = 200$ Å. (b) A plot of ν_0 as a function of k_y for a single quantum well. We chose $B_\parallel = 4\ T$; m^*, V_0, and $2a$ are the same as for (a).

width of the barrier between the wells is $b = 20$ Å, and the barrier height is $V_0 = 213$ meV. In figure 2(b), we plot the k_y-dispersion for fixed $B_\parallel = 4$ T and $k_z = 0$. The plots of the energy eigenvalues as functions of $B_\parallel$ and k_y in figures 2(a) and 2(b) show the anticrossing of

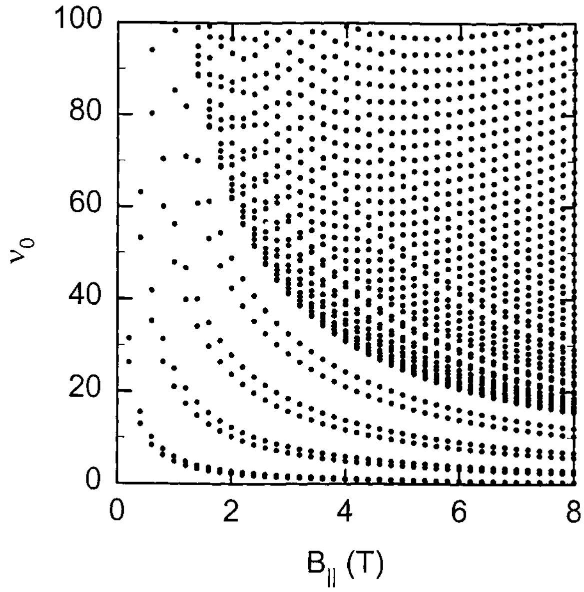

(a)

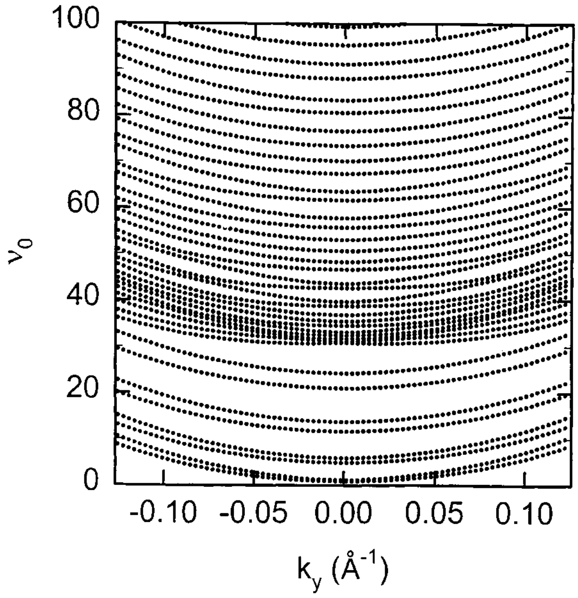

(b)

Figure 2. (a) A plot of the scaled energy eigenvalues $\nu_0 = E_j(k_y)/\hbar\omega_c - 1/2$ as a function of $B_{\parallel}$ for a double quantum well. Here, $k_y = 0$; m^* and the well width $2a$ are the same as in figure 1. We also choose $b = 20$ Å and $V_0 = 213$ meV here. (b) A plot of ν_0 as a function of k_y for a double quantum well. We chose $B_{\parallel} = 4\ T$; m^*, b, V_0, and $2a$ are the same as for (a).

the originally degenerate energy levels of the two QWs due to tunnelling in the presence of a magnetic field. The extended states above the top of the quantum well are clearly shown in figures 1 and 2. The anticrossing of the energy dispersion curves due to tunnelling between

QWs has been discussed by several authors (see, for example, reference [8]).

The energy spectrum for electrons in a superlattice in a parallel magnetic field has been discussed in the experimental work of Belle *et al* [14] and Maan [15] and in the theoretical paper by Brey *et al* [16], dealing with tunnelling in parallel magnetic fields. Some calculations making use of these results for the electron spectra of multi-quantum-well structures in parallel magnetic fields should be carried out to examine the role played by varying electron density and wave-function hybridization on the conductivity as the temperature is varied.

3. Out-of-plane electrical conductivity

Making use of the Kubo formula, the diagonal parts of the static conductivity at finite temperatures T are given by [17]

$$\sigma_{\mu\mu} = \int \mathrm{d}E \left[\frac{\mathrm{d}f_0(E)}{\mathrm{d}E}\right]\sigma_{\mu\mu}(E) \tag{3}$$

where $f_0(E)$ is the equilibrium Fermi–Dirac distribution function and

$$\sigma_{\mu\mu} = -\frac{\hbar e^2}{A}\sum_{\alpha,\alpha'}|V^{\mu}_{\alpha\alpha'}|^2 A_\alpha(E)A_{\alpha'}(E). \tag{4}$$

In this notation, the spectral function $A_\alpha(E) = \pi^{-1}\,\Im\, G^-_\alpha(E)$ where $G^-_\alpha(E) = [E - \epsilon_\alpha - \Sigma^-(E)]^{-1}$ with an effective self-energy determined by the self-consistency equation

$$\Sigma^-(E) = \sum_{\alpha,\alpha'} U^2_{\alpha\alpha'} G^-_\alpha(E). \tag{5}$$

Also, $U_{\alpha\alpha'}$ is a scattering matrix and α, α' stand for the labels $j, k_\parallel$ of the energy eigenstates. In the zero-temperature limit, $-\partial f_0(\varepsilon_\alpha)/\partial\varepsilon_\alpha$ is replaced by $\delta(\varepsilon_\alpha - \mu)$, so only the states with energy equal to the chemical potential contribute to the conductivity in equation (4) in this limit. The νth component of the velocity $\boldsymbol{V} = (-\mathrm{i}\hbar\boldsymbol{\nabla} + e\boldsymbol{A})/m^*$ matrix element is written as $V^\nu_{\alpha\beta}$. Setting $\mu = x$ and $\nu = x$, we obtain the static out-of-plane conductivity $\sigma_\perp = \sigma_{xx}$ which depends on

$$V^x_{jj'}(k_y) = \frac{-\mathrm{i}\hbar}{m^*}\int \mathrm{d}x\ \phi_{jk_y}(x)\,\frac{\partial}{\partial x}\phi_{j'k_y}(x). \tag{6}$$

We take a simple approximation for the self-energy:

$$\Sigma_\alpha(E) = \sum_{\alpha'} U^2_{\alpha\alpha'} G_{\alpha'}(E). \tag{7}$$

Setting the scattering matrix $U_{\alpha\alpha'} = U$, independent of the band index, the self-energy then becomes independent of the subscript α. Let $\Sigma^-_\alpha(E - \mathrm{i}0^+) = M(E) + \mathrm{i}\Gamma(E)$. Then with $\epsilon_\alpha = E_j(\boldsymbol{k}_\parallel) = E_j(k_y) + \hbar^2 k_z^2/2m^*$, the k_z-integration in equation (7) can be done analytically. Taking $U^2 = 2\Gamma_0\hbar^2/(Am^*)$, where A is the cross-sectional area, we obtain after a straightforward calculation

$$\Sigma(E) = -\frac{2\mathrm{i}\Gamma_0}{\pi}\left(0.190\frac{m_e}{m^*}\right)^{1/2}\sum_j\int_{-\infty}^{\infty}\mathrm{d}(k_y \times 100\ \text{Å}) \times\left[\frac{1}{\sqrt{|Z_{jk_y}(E)| + \Re\, Z_{jk_y}(E)} + \mathrm{i}\sqrt{|Z_{jk_y}(E)| - \Re\, Z_{jk_y}(E)}}\right] \tag{8}$$

where $\Sigma(E) = E - E_j(k_y) - Z_{jk_y}(E)$ and the energy in equation (8) is measured in meV. For a given density, n_{2D} for the 2DEG is $n_{2D} = \int \mathrm{d}E\ f_0(E)D(E)$ where $D(E)$ is the density of states.

We now present numerical results for the out-of-plane conductivity $\sigma_\perp$ of the SQW and DQW in a parallel magnetic field. In figure 3, we plot $\sigma_\perp$ as a function of temperature for a fixed in-plane magnetic field $B_\parallel = 2$ T and a sheet density of $n_{2D} = 2.0 \times 10^{11}$ cm^{-2}; the Fermi temperature is $T_F = 83$ K. In these calculations, all the energy eigenvalues obtained by solving the Schrödinger equation (1) were employed. The results show that in the low-temperature range, $\sigma_\perp$ is almost the same for both the SQW and the DQW and $\sigma_\perp \sim T^{-1}$ like for a metal. As the temperature is increased, $\sigma_\perp$ rises more rapidly for the DQW compared with the single well. Figure 4 is a plot of $\sigma_\perp$ with $B_\parallel = 2$ T but for a smaller density $n_{2D} = 1.0 \times 10^{10}$ cm^{-2}; these results show that at low temperature ($T < 0.2$ K), the behaviour of $\sigma_\perp$ for the SQW differs from that for the DQW. When the density is fixed but the magnetic field is reduced from $B_\parallel = 2$ T to 0.5 T, $\sigma_\perp$ increases more rapidly with temperature for the smaller magnetic field for either the SQW or the DQW when $T \gtrsim 20$ K, but below this temperature the curves are almost the same. When the width of the barrier between the QWs is decreased, the tunnelling is reduced and the value of $\sigma_\perp$ is decreased for a fixed magnetic field. Tunnelling between the QWs thus enhances $\sigma_\perp$. At low temperatures, the variation of $\sigma_\perp$ with density is consistent with the fact that the kinetic energy dominates the potential energy when the electron density is increased. Also, the relative importance of many-body interactions depends on temperature. This is why at low temperatures the variation of $\sigma_\perp$ is determined by the electron density. In figure 5, we plot $\sigma_\perp$ for a DQW with $B_\parallel = 2$ T and a density of $n_{2D} = 1.0 \times 10^{10}$ cm^{-2}, the same as for figure 4. The purpose of this figure is to demonstrate the role played by the states above the top of the barrier, as the temperature varies.

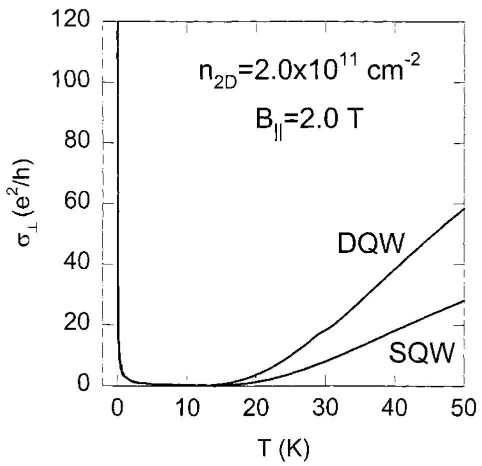

Figure 3. $\sigma_\perp = \sigma_{xx}$ (in units of e^2/h) is plotted as a function of temperature for a single quantum well and a double quantum well with $B_\parallel = 2$ T and $n_{2D} = 2.0 \times 10^{11}$ cm^{-2}. The electron effective mass is $m^* = 0.0667\ m_e$, where m_e is the free-electron mass. The barrier height is $V_0 = 213$ meV and the well width is $2a = 200$ Å. The separation between the two wells for the DQW structure is $b = 20$ Å and the scattering matrix $U = 3.0$ meV.

The metal–insulator transition in a 2D hole gas, as the density is varied, has been reported recently [18–20] at $B = 0$ for 2D systems, as evidence for the existence of a metallic state in 2D systems with low disorder. In these experiments, it is the in-plane conductivity which is measured. Experiments on high-mobility silicon inversion layers [21] have also shown a transition from insulating to metallic behaviour as the carrier density is increased, characterized by an exponential decrease in resistance as temperature is reduced. The results that we have presented in this paper for the out-of-plane conductivity of the double-QW structure show that

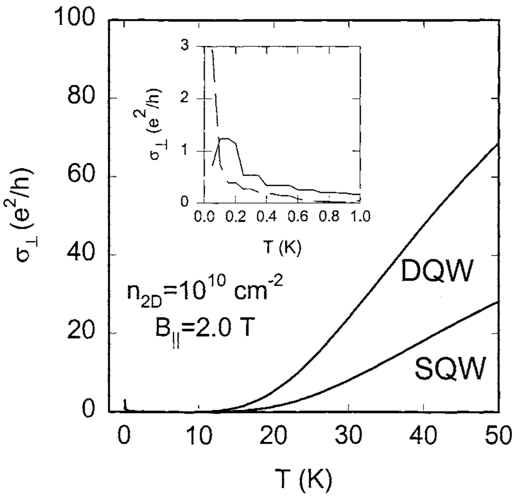

Figure 4. As figure 3, but for $n_{2D} = 1.0 \times 10^{10}$ cm^{-2}. The inset is a magnification of the results at low temperature with the solid line corresponding to the single quantum well and the dashed line to the double quantum well.

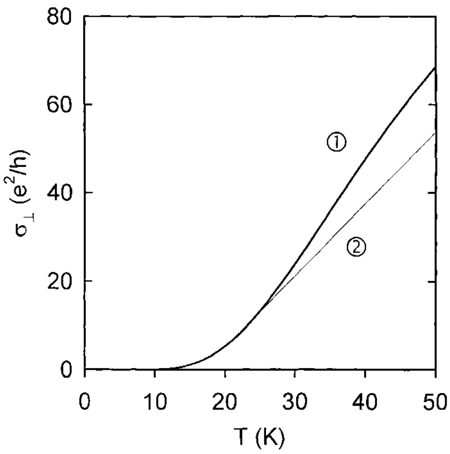

Figure 5. Comparison of the results for $\sigma_\perp$ for a DQW (1) when the states above the top of the barrier are included and (2) when these states are neglected and only the confined energy states are included in the calculation. The magnetic field $B_\parallel = 2$ T and $n_{2D} = 1.0 \times 10^{10}$ cm^{-2}. The electron effective mass is $m^* = 0.0667\ m_e$, where m_e is the free-electron mass. The barrier height is $V_0 = 213$ meV and the well width is $2a = 200$ Å. The separation between the two wells is $b = 20$ Å and the scattering matrix $U = 3.0$ meV.

in a parallel magnetic field the behaviour of the conductivity as the temperature is decreased depends on the carrier concentration. There has been no equivalent observation for the strongly coupled 2D systems but the results reported here for $\sigma_\perp$ show that the transition from metallic-like to insulating behaviour also has an interesting dependence on the electron density. The additional inter-layer electron–electron scattering introduces phase incoherence in strongly coupled QWs making it possible for $\sigma_\perp$ to reveal these interesting transport properties.

4. Concluding remarks

In conclusion, we have calculated the dispersion relation for the energy eigenvalues in a SQW and a DQW system in an in-plane magnetic field. For the double quantum well, the energy eigenvalues include tunnelling between the quantum wells, and display the anticrossing features for the energy dispersion curves for the two QWs. The out-of-plane conductivity was calculated as a function of temperature. The higher-lying states are important in these calculations because at finite temperature the Fermi distribution function picks up a contribution not only from the confined states within the QW but also from the states above the top of the barrier. We show that in the low-temperature regime, the behaviour of $\sigma_\perp$ at high density differs from that at low density.

There has been no experimental work reported so far in the literature on the metal–insulator transition, for coupled 2DEG layers. Strongly coupled QWs differ from an isolated well in the additional inter-layer electron–electron scattering which introduces phase incoherence. In the work by Kravchenko *et al* [21] a very interesting change in scattering occurs as the density is varied, but at low temperatures the resistance saturates and the log corrections return and all states are localized. We hope that the work reported here will stimulate experiments on coupled 2D systems in a parallel magnetic field.

Acknowledgments

The author acknowledges the support in part from a NATO Grant No CRG-972117 (US–UK Collaborative Grant), the City University of New York PSC-CUNY grants No 664279 and No 669456, as well as the Minority Biomedical Research Support (MBRS) grant No GM56945-01 from the NIH.

References

[1] Arnone D D, Marlow T P, Foden C L, Linfield E H, Ritchie D A and Pepper M 1997 *Phys. Rev.* B **56** R4340
[2] Das Sarma S and Hwang E H 1998 *Phys. Rev. Lett.* **81** 4216
[3] Gumbs G and Aĭzin G R 1995 *Phys. Rev.* B **51** 7074
Aĭzin G R and Gumbs G 1995 *Phys. Rev.* B **52** 1890
[4] Boebinger G S, Jiang H W, Pfeiffer L N and West K W 1990 *Phys. Rev. Lett.* **64** 1793
[5] Simmons J A, Lyo S K, Klem J F, Sherwin M E and Wendt J R 1993 *Phys. Rev.* B **47** 15 741
[6] Simmons J A, Lyo S K, Harff N E and Klem J F 1994 *Phys. Rev. Lett.* **73** 2256
[7] Simmons J A, Harff N E and Klem J F 1995 *Phys. Rev.* B **51** 11 156
[8] Lyo S K 1994 *Phys. Rev.* B **50** 4965
Lyo S K 1995 *Phys. Rev.* B **51** 11 160
[9] Rainer G, Smoliner J, Gornik E, Böhm G and Weimann G 1995 *Phys. Rev.* B **51** 17 642
[10] Zheng L and MacDonald A H 1993 *Phys. Rev.* B **47** 10 619
[11] Gumbs G 1996 *Phys. Rev.* B **54** 11 354
[12] Erdélyi A 1981 *Higher Transcendental Functions* vol II (Malabar, FL: Krieger) p 122
[13] *Handbook of Mathematical Functions* 1970 ed M Abramowitz and I A Stegun (New York: Dover) p 685
[14] Belle G, Maan J C and Weimann G 1986 *Surf. Sci.* **170** 611
[15] Maan J C 1987 *Festkörperprobleme (Advances in Solid State Physics)* vol 27, ed O Madelung (New York: Pergamon) p 137
[16] Brey L, Platero G and Tejedor C 1988 *Phys. Rev.* B **38** 9649
[17] Zhang C and Gerhardts R R 1990 *Phys. Rev.* **41** 12 850
[18] Hamilton A R, Simmons M Y, Pepper M, Linfield E H, Rose P D and Ritchie D A 1998 *Phys. Rev. Lett.* **82** 1542
[19] Coleridge P T, Williams R L, Feng Y and Zawadzki P 1997 *Phys. Rev.* B **56** R12 764
[20] Hanein Y, Meirav U, Shakar D, Li C C, Tsui D C and Shtrikman H 1998 *Phys. Rev. Lett.* **80** 1288
[21] Kravchenko S V, Kravchenko G V, Furneaux J E, Pudalov V M and D'Iorio M M 1994 *Phys. Rev.* B **50** 8039
Kravchenko S V, Mason W E, Bowker G E, Furneaux J E, Pudalov V M and D'Iorio M M 1995 *Phys. Rev.* B **51** 7038